AIP | Review of Scientific Instruments

Frequency-modulated atomic force microscopy operation by imaging at the frequency shift minimum: The dip-df mode

Sebastian Rode, Martin Schreiber, Angelika Kühnle, and Philipp Rahe

Citation: Review of Scientific Instruments **85**, 043707 (2014); doi: 10.1063/1.4871436
View online: http://dx.doi.org/10.1063/1.4871436
View Table of Contents: http://scitation.aip.org/content/aip/journal/rsi/85/4?ver=pdfcov
Published by the AIP Publishing

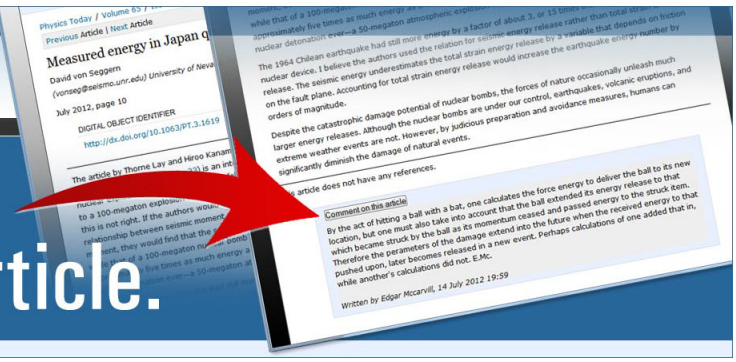

Frequency-modulated atomic force microscopy operation by imaging at the frequency shift minimum: The dip-df mode

Sebastian Rode,[a] Martin Schreiber,[b] Angelika Kühnle,[b] and Philipp Rahe[c]
Institut für Physikalische Chemie, Fachbereich Chemie, Johannes Gutenberg-Universität Mainz, Duesbergweg 10-14, 55099 Mainz, Germany

(Received 22 November 2013; accepted 3 April 2014; published online 28 April 2014)

In frequency modulated non-contact atomic force microscopy, the change of the cantilever frequency (Δf) is used as the input signal for the topography feedback loop. Around the $\Delta f(z)$ minimum, however, stable feedback operation is challenging using a standard proportional-integral-derivative (PID) feedback design due to the change of sign in the slope. When operated under liquid conditions, it is furthermore difficult to address the attractive interaction regime due to its often moderate peakedness. Additionally, the Δf signal level changes severely with time in this environment due to drift of the cantilever frequency f_0 and, thus, requires constant adjustment. Here, we present an approach overcoming these obstacles by using the derivative of Δf with respect to z as the input signal for the topography feedback loop. Rather than regulating the absolute value to a preset setpoint, the slope of the Δf with respect to z is regulated to zero. This new measurement mode not only makes the minimum of the $\Delta f(z)$ curve directly accessible, but it also benefits from greatly increased operation stability due to its immunity against f_0 drift. We present isosurfaces of the Δf minimum acquired on the calcite $CaCO_3(10\bar{1}4)$ surface in liquid environment, demonstrating the capability of our method to image in the attractive tip-sample interaction regime. © *2014 AIP Publishing LLC*. [http://dx.doi.org/10.1063/1.4871436]

I. INTRODUCTION

Over the last decades, atomic force microscopy (AFM) has proven to be one of the most useful techniques for resolving surface structures from the mesoscopic scale down to the atomic level in fields such as surface science, biochemistry, or materials science.[1] Especially in the frequency-modulated (FM) non-contact (NC) mode, atomic resolution is nowadays routinely achieved when operating the AFM under ultra-high vacuum conditions.[2] Recently, the success of atomic-scale imaging has been transferred to the liquid environment,[3] demonstrating atomic-resolution imaging on surfaces such as, e.g., mica(001),[4] calcite(104),[5–8] aragonite(001),[9] calcium difluorite[10] as well as $LiNbO_3(00\bar{1})$,[11] and, furthermore, high-resolution imaging on molecular systems.[12]

These achievements have only been possible after carefully optimizing the experimental setup for increasing the signal-to-noise ratio.[3,13] However, operating FM NC-AFM in liquid environment still requires a delicate adjustment of the scanning parameters compared to other AFM modes in different environments. Here we note that, first, usually large drift not only distorts the acquired images in all three spatial directions,[14] but additionally causes a severe change of the cantilever reference frequency in time.[15] This drift is likely caused by thermal fluctuations of the AFM system, by an evaporation of the liquid or by stray excitations of the surrounding environment. In principle, each of these issues can be addressed individually by a careful experimental design.[3,4,9,16–18] Second, finding a suitable Δf setpoint for imaging in the repulsive regime can be delicate and imaging in this regime might significantly wear off the scanning probe tip. Third, imaging in liquids is typically performed in the repulsive tip-sample interaction regime. This is due to the fact that in the attractive regime the frequency shift signal does often not largely deviate from the noise level, even at the largest negative values. As a consequence, the attractive regime is hardly accessible. The latter statement is especially true when considering drift in f_0, easily causing absolute frequency drifts that are larger than the $\Delta f(z)$ minimum. This possibly brings the feedback loop into an instable regime. Last, the amplitude spectrum usually resembles the well-known "forest of peaks," where numerous resonances besides the cantilever resonance are apparent due to the environment.[19–21] This issue has been addressed by using direct actuation methods such as magnetic,[22] photothermal,[16,23] and electrostatic[20,24] excitation.

Here, we present a new measurement mode where the tip-sample distance is adjusted such that imaging is always performed at the minimum of the $\Delta f(z)$ curve. The existence of a minimum in the $\Delta f(z)$ curve is a prerequisite for using this measurement mode. This mode is introduced as a promising strategy addressing the aforementioned challenges and providing most practical solutions to them: First, it is immune against drift of the cantilever reference frequency as we regulate on the z derivative of the Δf signal. Second, the setpoint for the distance feedback loop is well-defined and does not require any adjustment, and third, it images the sample system in the overall attractive regime.

[a]Present address: SmarAct GmbH, Schuette-Lanz-Strasse 9, 26135 Oldenburg, Germany.
[b]URL: http://www.self-assembly.uni-mainz.de.
[c]Present address: Department of Physics and Astronomy, The University of Utah, 115 South 1400 West, Salt Lake City, UT 84112, USA; Electronic mail: rahe@uni-mainz.de.

Imaging in the overall attractive regime is gentler than imaging in the repulsive regime. Consequently, we expect our measurement mode to reduce modifications of sensitive materials such as biological samples or other soft matter.

II. PRINCIPLE

The main measurement signal in FM NC-AFM is the frequency shift Δf, defined by $\Delta f = f - f_0$.[25] Here, f_0 is the frequency of the cantilever oscillating without any tip-sample interaction, which changes to f when the tip is interacting with the sample. The frequency shift Δf is related to the tip-sample interaction force F_{ts} by convolving the force with a weighting function resembling the cantilever oscillation.[26] The frequency shift $\Delta f(z)$ along the tip-sample distance z usually follows a curve qualitatively similar to the interaction force as depicted in Fig. 1 (solid green curve): Far away from the surface in the long-range regime, the interaction is basically zero. Upon approach, at first long-range attractive van der Waals and electrostatic interactions are the dominant interactions, leading to a negative shift in Δf. A minimum is passed when repulsive interactions become more pronounced upon reducing the tip-sample distance and, finally, repulsive interactions dominate, typically when the frequency shift is positive.[27]

In Fig. 1, the derivative $\Delta f'(z)$ (dashed orange curve) is presented in addition to the $\Delta f(z)$ curve (solid green). The derivative exhibits a maximum at the inflection point of the $\Delta f(z)$ curve and, most importantly, has its root at the $\Delta f(z)$ minimum position. The method described here uses this derivative as the input signal for the topography feedback loop. When keeping the $\Delta f'$ setpoint at zero, the topography signal will map an isosurface of $\Delta f(z) = \text{min}$, i.e., the vertical position of the $\Delta f(z)$ minimum for each lateral point. This specific position along the $\Delta f(z)$ curve is usually inaccessible with a feedback relying on a monotonic behavior due to the change in sign of the slope in the $\Delta f(z)$ curve.

Experimentally, the derivative is directly accessible using a well-known lock-in principle: the z piezo signal is modulated with frequency f_{mod} and amplitude A_{mod}. The amplitude and phase of the resulting oscillation in Δf are then measured using a lock-in amplifier. The technical implementation is presented in Sec. III.

Modulation techniques of the Z position have been used before to rapidly discriminate between different chemical species from the slope of $\Delta f(z)$ curves.[28] Furthermore, Z modulation has been used to quickly recover the nonlinear $\Delta f(z)$ curve from measuring the higher harmonics in the frequency shift signal.[29]

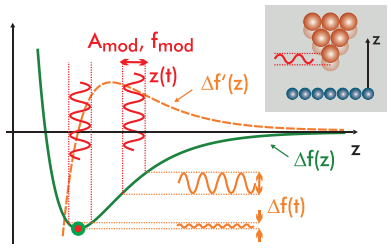

FIG. 1. Schematic $\Delta f(z)$ interaction curve for FM NC-AFM experiments (solid green) and corresponding derivative $\Delta f'(z)$ curve (dashed orange). The trajectory of the tip $z(t)$ and the resulting $\Delta f(t)$ signal are included in solid red and orange, respectively.

III. IMPLEMENTATION

For implementing our "dip-df" mode, where the tip-sample distance is regulated to the minimum dip of the $\Delta f(z)$ curve, an oscillating signal with amplitude A_{mod} and frequency f_{mod} is added to the high-voltage z signal from the scan controller. This leads to a modulation of the tip-sample distance, which, in turn, results in a modulation of the frequency shift Δf.[29] As depicted in Fig. 1, this oscillation along the z direction results in an oscillation of the Δf signal if the slope of the $\Delta f(z)$ curve differs from zero, i.e., within the sample range. The amplitude of this oscillation in the Δf channel is dependent on the slope of the $\Delta f(z)$ interaction and approaches zero at the $\Delta f(z)$ minimum position. As the phase between the z oscillation signal and the Δf oscillation changes by 180° when passing the $\Delta f(z)$ minimum, in addition the sign of the slope is readily available. Technically, the amplitude including the 180° phase shift when passing the minimum is easily detected using the in-phase signal of a lock-in amplifier.

Fig. 2 depicts the technical implementation of the dip-df method. Only two changes are necessary compared to a standard FM NC-AFM setup: First, a sinusoidal signal is added to the z signal generated by the scan controller and, second, the in-phase (X) signal of the lock-in amplifier is fed into the topography feedback loop as input signal. The Δf signal from the PLL is then used as the input signal for the lock-in amplifier.

The signal summation is realized by adding the sinusoidal signal from a frequency generator to the scan controller signal. We used a mass-decoupled concept for the low-noise summation of low-voltage to high-voltage signals as described in Ref. 30.

As PLL and lock-in amplifier we used an HF2 device from Zurich Instruments (Zurich, Switzerland). For the z modulation, a frequency in the range of $f_{\text{mod}} = 6$–8 kHz and an amplitude of about $A_{\text{mod}} = 100$ mV were used. This amplitude corresponds to a physical amplitude of about 1.5 Å using the calibration for the herein used modified Bruker Multimode V atomic force microscope.[13] The PLL was set to a bandwidth slightly larger than f_{mod}, while the response of the z feedback loop was set significantly slower. The time constant of the lock-in amplifier was in the order of 30 μs. For regular FM NC-AFM experiments, an easyPLL plus (Nanosurf, Neuchâtel, Switzerland) controller and detector with a bandwidth of 1300 Hz was used in parallel for practical reasons. The reference frequency was determined from the excitation spectrum far away from the sample surface.

The dip-df method implementation and all experiments were performed using a modified Bruker Multimode V AFM, optimized for low-noise performance in the FM NC-AFM mode.[13] Gold coated p-doped silicon cantilevers (type PPP-NCH-AuD from Nanosensors, Neuchâtel, Switzerland) with typical frequencies of around 160 kHz in liquid were operated at amplitudes of around 1–2 nm. The microscope is enclosed by a home-built measurement chamber. The temperature of the entire compartment is controlled by

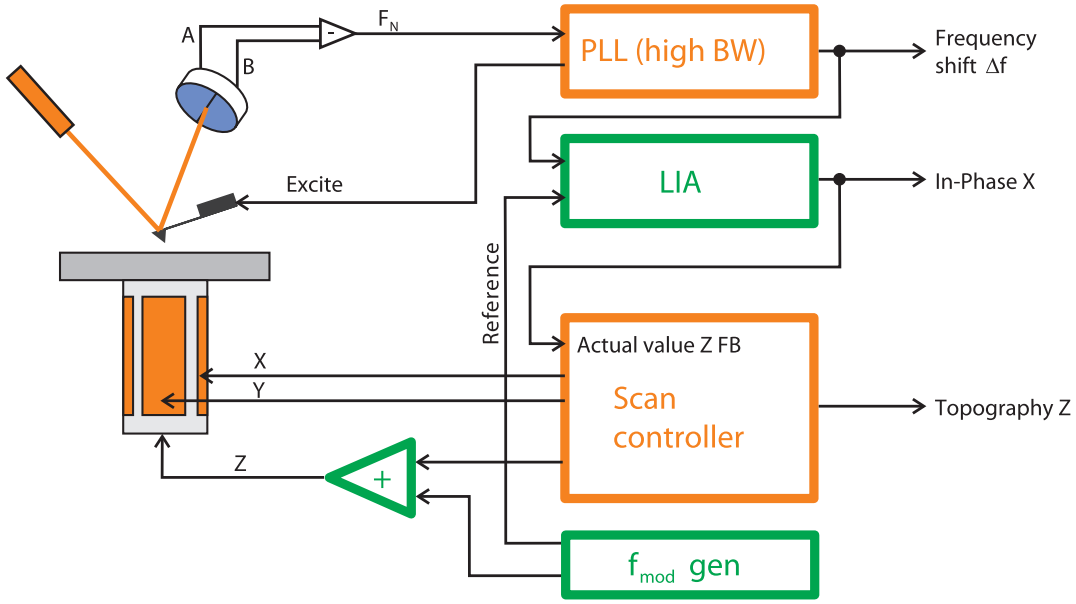

FIG. 2. Technical implementation of the dip-df AFM mode. Components additional to a standard FM NC-AFM setup are depicted in green: Lock-in amplifier (LIA), generator for the oscillation signal (f_{mod} gen), and high-voltage summation circuit (+). The phase-locked loop (PLL) is set to a bandwidth larger than f_{mod}.

current-regulated resistors, allowing for temperatures in the range of 30–50 °C. The resulting temperature stability of this setup is about ±0.5 °C.[13]

As substrate, we used the calcite $(10\bar{1}4)$ surface,[31] the most stable cleavage plane of the most stable polymorph of calcium carbonate $CaCO_3$. Pristine surfaces were created by cleaving a bulk crystal in air and immediately introducing it into the liquid cell. The liquid cell was filled with deionized (Milli-Q) water. Following this preparation routine allows for achieving atomic-resolution imaging of the calcite substrate using FM NC-AFM as has been demonstrated before.[5]

IV. DEMONSTRATION

Exemplary $\Delta f(z)$ curves acquired on the $CaCO_3(10\bar{1}4)$ surface are reproduced in Fig. 3. These curves present a single minimum where the dip-df approach can be applied in a straightforward manner. On calcite, recent experiments have revealed the different hydration layers on the surface,[8] leading to multiple minima in the $\Delta f(z)$ curve. Under the assumption that the separation of the minima along z is larger than the modulation amplitude z_{mod} and that the signal-to-noise ratio allows for a clear distinction of the multiple zero positions in $\Delta f'$, we can speculate that the dip-df mode might even distinguish between these minima. In contrast, we expect to average the substructure and lock to the global minimum by using large oscillation amplitudes z_{mod}. As mentioned before, the peak of the attractive regime can be very shallow compared to the noise level as is clearly visible. Especially when considering drift of f_0 in the order of a several Hz/min, the minimum is hardly accessible experimentally within the timespan necessary for imaging. Thus, imaging is usually performed in the steep regime of negative slope. Furthermore, we find from this curve a difference in height in the order of 5 Å between imaging at positive frequency shift and imaging at the minimum. Although measuring in the repulsive regime might be necessary to achieve atomic-scale resolution, it is also expected to lead to instabilities and potential damages on tip or sample.

Using regular FM NC-AFM in Δf feedback, we approach and image a $CaCO_3(10\bar{1}4)$ surface on a large scale. Figure 4(a) presents the topography image acquired in the negative $\Delta f(z)$ slope regime at a setpoint of about +100 Hz. After completing this image, the z modulation is switched on while the height feedback loop is still engaged. The phase offset of the lock-in amplifier is adjusted such that the in-phase signal is maximized. Depending on the input sign of the distance feedback loop configuration, an inversion (phase shift of 180°) of the signal might be necessary. The tip is retracted after this adjustment, the distance feedback loop is frozen and its input signal is changed from Δf to the lock-in in-phase signal. The $\Delta f(z)$ curve is constant at large tip-sample distances, resulting in a zero in-phase and amplitude signal of the lock-in amplifier. Consequently, in order to engage to the sample after reactivating the feedback loop, a small offset added to the

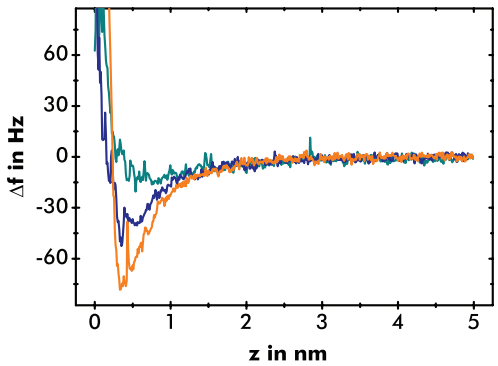

FIG. 3. Representative $\Delta f(z)$ curves acquired on the $CaCO_3(10\bar{1}4)$ surface for different tip terminations and different surface sites. In most cases, the attractive regime is hardly accessible due to the small peakedness compared to the noise level. All curves have been shifted along the vertical axis to match zero at $z = 5$ nm.

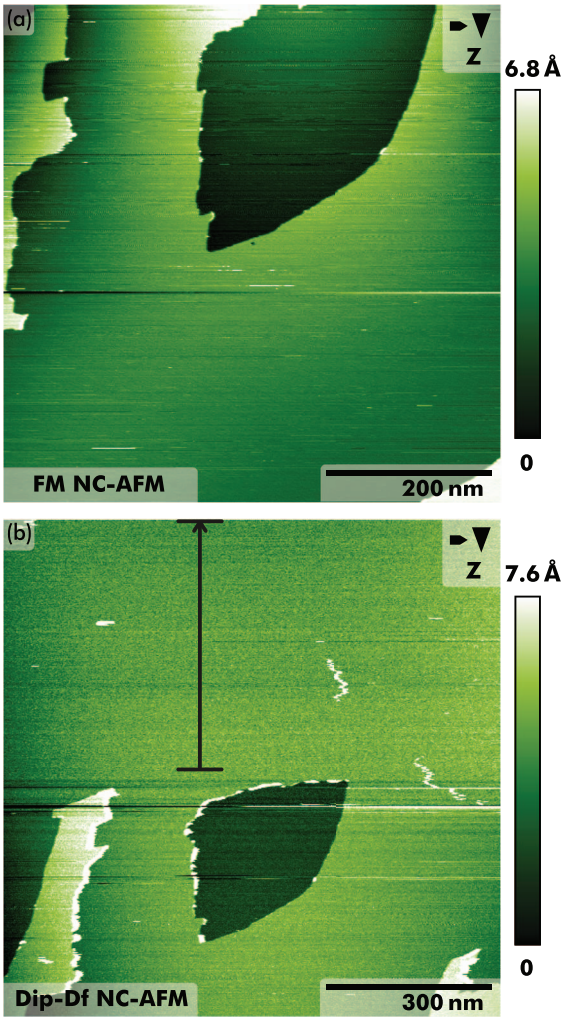

FIG. 4. (a) Regular FM NC-AFM mode using the frequency shift Δf as input for the topography feedback loop. (b) Dip-df AFM mode using the derivation $\Delta f'(z)$ as input signal for the topography feedback loop with setpoint zero. The resulting image, thus, represents the isoplane of minimum Δf. Both images were compensated for vertical thermal drift, scanner hysteresis, sample tilt, and tip changes by a line-by-line and second order polynomial correction. The position of the line profile extracted from the frequency shift channel (see Fig. 5) is marked by a black line. Parameters for both images: $512 \times 512\,\text{pixel}^2$ at 1 line/s (forward and backward scan).

in-phase lock-in signal is usually necessary. After stabilizing the tip position close to the surface, this offset is set to zero for stabilizing the tip precisely at the minimum of the $\Delta f(z)$ curve. We note that the intermediate maximum of the $\Delta f'(z)$ curve is not causing feedback instabilities and can easily be passed as we regulate on the zero position.

Figure 4(b) presents the topography channel when operating in the dip-df mode. The topography now directly resembles the isosurface of the $\Delta f(z)$ minimum position. The data acquired in the regular FM mode and the dip-df mode are acquired at the same sample position, the lateral movement is caused by drift. In both images, calcite step edges and an etch pit due to calcite dissolution in water are resolved.

By comparing the two topography images (see Fig. 4), we observe a slight increase in the topography signal noise for the dip-df mode. Although the RMS noise in the topography signal can by itself already be subject to the feedback

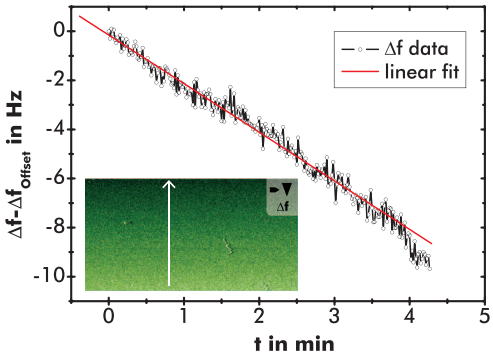

FIG. 5. Averaged line profile extracted at the indicated position in Fig. 4(b) from the regular Δf channel (shown in the inset, see also Fig. 4(b)). The horizontal axis has been rescaled to depict the elapsed time. A linear regression directly reveals a drift of the cantilever reference frequency f_0 of about 2 Hz/min.

loop characteristics, we especially note that the dip-df method operates in a conventionally not reachable interaction regime around the Δf minimum. Compared to the repulsive regime, the absolute forces are smaller around the minimum position, explaining the possibility for larger noise under the same effective measurement conditions.

To illustrate the robustness of this technique against drift of the cantilever frequency f_0, we present in Fig. 5 a line profile extracted from the Δf channel acquired simultaneously to Fig. 4(b). A linear fit reveals a drift of about 2 Hz/min, which would severely hinder measuring in the attractive regime after a few minutes. We also note that the dip-df technique delivers a strategy to distinguish between drift along the spatial z axis and the cantilever frequency f_0.

V. CONCLUSION

We presented a new AFM measurement mode, which allows for NC-AFM experiments at tip-sample distances corresponding to the $\Delta f(z)$ minimum, resulting in a map of $\Delta f = \min$. Especially when using FM NC-AFM in liquid environment, this *dip-df* mode is a helpful extension to the regular FM mode. It circumvents the problem of drift in the cantilever reference frequency f_0 and allows for imaging in the attractive tip-sample interaction regime. We successfully imaged the calcite $CaCO_3(10\bar{1}4)$ surface in this mode revealing step edges and etch pits.

Especially on soft or sensitive sample systems, we account this mode to be beneficial compared to the regular repulsive FM NC-AFM mode in liquids due to reduced tip-sample interaction forces while imaging.

ACKNOWLEDGMENTS

We thank Christoph Marutschke, Holger Adam, and Steffi Klassen for their most helpful experimental assistance, Christopher Hauke for naming the method, and Sadik Hafizovic for most helpful support with the HF2 configuration.

[1]H.-J. Butt, B. Cappella, and M. Kappl, Surf. Sci. Rep. **59**, 1 (2005).
[2]C. Barth, A. S. Foster, C. R. Henry, and A. L. Shluger, Adv. Mater. **23**, 477 (2011).
[3]T. Fukuma, M. Kimura, K. Kobayashi, K. Matsushige, and H. Yamada, Rev. Sci. Instrum. **76**, 053704 (2005).

[4]T. Fukuma, K. Kobayashi, K. Matsushige, and H. Yamada, Appl. Phys. Lett. **87**, 034101 (2005).
[5]S. Rode, N. Oyabu, K. Kobayashi, H. Yamada, and A. Kühnle, Langmuir **25**, 2850 (2009).
[6]M. Ricci, P. Spijker, F. Stellacci, J.-F. Molinari, and K. Votchovsky, Langmuir **29**, 2207 (2013).
[7]H. Imada, K. Kimura, and H. Onishi, Chem. Phys. **419**, 193 (2013).
[8]H. Imada, K. Kimura, and H. Onishi, Langmuir **29**, 10744 (2013).
[9]Y. Araki, K. Tsukamoto, N. Oyabu, K. Kobayashi, and H. Yamada, Jpn. J. Appl. Phys. **51**, 08KB09 (2012).
[10]N. Kobayashi, S. Itakura, H. Asakawa, and T. Fukuma, J. Phys. Chem. C **117**, 24388 (2013).
[11]S. Rode, R. Hölscher, S. Sanna, S. Klassen, K. Kobayashi, H. Yamada, W. G. Schmidt, and A. Kühnle, Phys. Rev. B **86**, 075468 (2012).
[12]M. Schreiber, M. Eckardt, S. Klassen, H. Adam, M. Nalbach, L. Greifenstein, F. Kling, M. Kittelmann, R. Bechstein, and A. Kühnle, Soft Matter **9**, 7145 (2013).
[13]S. Rode, R. Stark, J. Lübbe, L. Tröger, J. Schütte, K. Umeda, K. Kobayashi, H. Yamada, and A. Kühnle, Rev. Sci. Instrum. **82**, 073703 (2011).
[14]P. Rahe, R. Bechstein, and A. Kühnle, J. Vac. Sci. Technol. B **28**, C4E31 (2010).
[15]F. J. Giessibl, Rev. Mod. Phys. **75**, 949 (2003).
[16]H. Adam, S. Rode, M. Schreiber, K. Kobayashi, H. Yamada, and A. Kühnle, Rev. Sci. Instrum. **85**, 023703 (2014).
[17]N. Umeda, S. Ishizaki, and H. Uwai, J. Vac. Sci. Technol. B **9**, 1318 (1991).
[18]G. C. Ratcliff, D. A. Erie, and R. Superfine, Appl. Phys. Lett. **72**, 1911 (1998).
[19]T. E. Schäffer, J. P. Cleveland, F. Ohnesorge, D. A. Walters, and P. K. Hansma, J. Appl. Phys. **80**, 3622 (1996).
[20]K.-I. Umeda, K. Kobayashi, K. Matsushige, and H. Yamada, Appl. Phys. Lett. **101**, 123112 (2012).
[21]X. Xu and A. Raman, J. Appl. Phys. **102**, 034303 (2007).
[22]W. Han, S. M. Lindsay, and T. Jing, Appl. Phys. Lett. **69**, 4111 (1996).
[23]A. Labuda, K. Kobayashi, Y. Miyahara, and P. Grütter, Rev. Sci. Instrum. **83**, 053703 (2012).
[24]K.-I. Umeda, N. Oyabu, K. Kobayashi, Y. Hirata, K. Matsushige, and H. Yamada, Appl. Phys. Express **3**, 065205 (2010).
[25]T. R. Albrecht, P. Grütter, D. Horne, and D. Rugar, J. Appl. Phys. **69**, 668 (1991).
[26]F. J. Giessibl, Phys. Rev. B **56**, 16010 (1997).
[27]P. Rahe, R. Bechstein, J. Schütte, F. Ostendorf, and A. Kühnle, Phys. Rev. B **77**, 195410 (2008).
[28]Y. Sugimoto, T. Namikawa, M. Abe, and S. Morita, Appl. Phys. Lett. **94**, 023108 (2009).
[29]S. Kawai, S. Hafizovic, T. Glatzel, A. Baratoff, and E. Meyer, Phys. Rev. B **85**, 165426 (2012).
[30]P. Rahe, J. Schütte, W. Schniederberend, M. Reichling, M. Abe, Y. Sugimoto, and A. Kühnle, Rev. Sci. Instrum. **82**, 063704 (2011).
[31]P. Rahe, J. Schütte, and A. Kühnle, J. Phys.: Condens. Matter **24**, 084006 (2012).